Strip-Like Laminations Influence on Bending and Bonding Performance of Yellow Birch Glulam

João Vítor Felippe Silva [a], Pierre Blanchet [a,*] and Marie Metten [b]

* Corresponding author: pierre.blanchet@sbf.ulaval.ca

DOI: 10.15376/biores.21.1.2215-2228

GRAPHICAL ABSTRACT

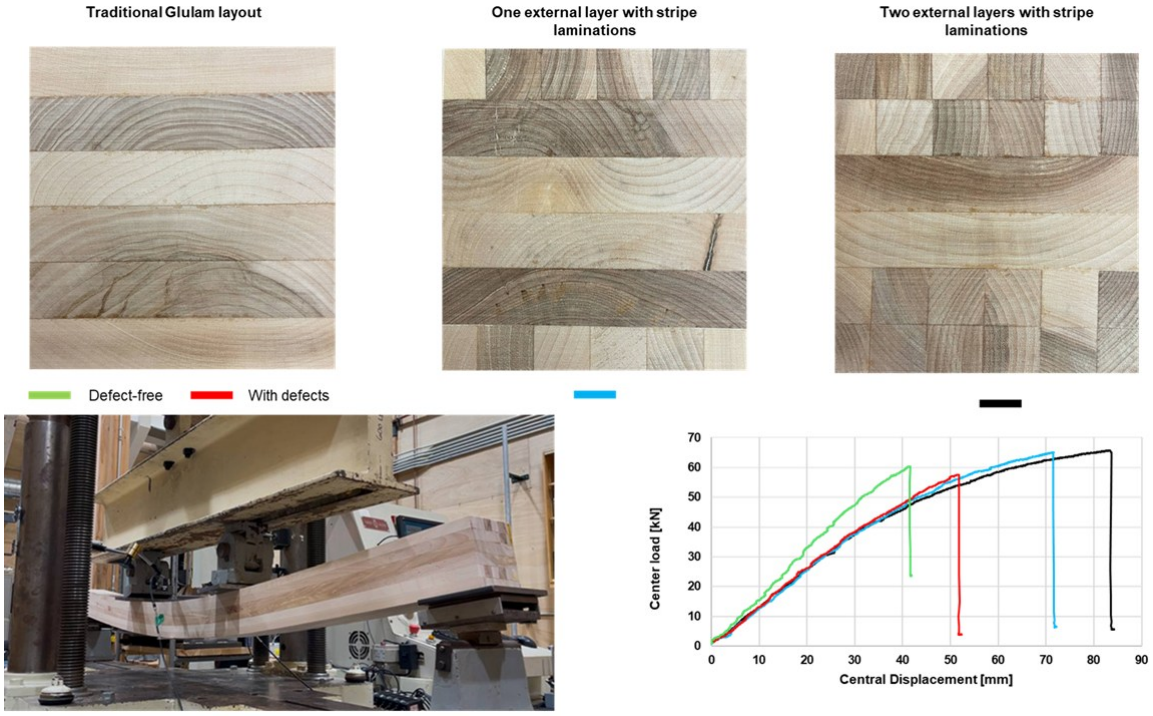

Strip-Like Laminations Influence on Bending and Bonding Performance of Yellow Birch Glulam

João Vítor Felippe Silva [a], Pierre Blanchet [a,*] and Marie Metten [b]

Strip-like laminations are wood lamellae formed by face-gluing small wood segments to reduce the effect of natural defects and enable the use of lower-grade timber. This technique offers a promising solution for transforming low-grade wood into solid products. However, its impact on full-scale structural components such as glulam beams has yet to be thoroughly assessed. This study investigated how external layers made of strip-like laminations affected glulam's bending properties and bonding performance. Grade No. 2 yellow birch (*Betula alleghaniensis* Britt.) was bonded with one-component polyurethane to fabricate six-layer glulam beams, with strip-like laminations placed on the outer layers. Mechanical testing, including four-point bending, block shear, and delamination, was conducted in accordance with North American standards. Results showed a one-third reduction in the variability of modulus of rupture (MOR), while maintaining comparable performance to traditional glulam configurations. Although apparent modulus of elasticity (MOE_{app}) was slightly lower and similar to beams containing visual defects, block-shear strength exceeded 90% approval. Some cases of delamination above 10% highlight opportunities for process refinement. These findings demonstrate the potential of strip-like laminations for improving material utilization and provide valuable insights for optimizing manufacturing strategies.

DOI: 10.15376/biores.21.1.2215-2228

Keywords: Delamination; Block-shear; Four-point bending; Hardwood

*Contact information: a: Département des sciences du bois et de la forêt, Université Laval, Québec, QC G1V 0A6 Canada; b: Département Sciences et Technologies, Haute École Robert Schuman, Rue Fontaine aux Mûres 13B B-6800, Libramont-Chevigny, Belgium; * Corresponding author: pierre.blanchet@sbf.ulaval.ca;*

INTRODUCTION

For millennia, wood has been a fundamental construction material due to its widespread availability, high adaptability, and renewable nature. To improve utilization efficiency and address the inherent variability of natural timber, engineered wood composites (EWPs), known for their designable structural properties and dimensional stability, have become increasingly prevalent in a wide range of architectural applications (Van Acker 2021). EWPs are manufactured by adhesively bonding multiple layers of wood-based components, such as veneers or lamellae, using structural adhesives.

Among EWPs, glued-laminated timber (glulam) stands out for its high strength-to-weight ratio and design flexibility, making it a preferred choice for structural applications such as beams, trusses, and bridges (Morin-Bernard *et al.* 2021; Boku *et al.* 2023). In industrial-scale manufacturing across North America, the primary raw material for glulam consists of softwood species, which are chosen for their favorable processing characteristics and consistent fiber properties (Van Acker 2021). In contrast, the use of

hardwood species remains limited due to the industry's relatively lower technical familiarity and processing experience with these usually denser and structurally complex materials (Konnerth *et al.* 2016; Subhani and Lui 2024).

In recent decades, the construction sector has shown growing interest in incorporating hardwood species into building applications, largely due to their superior mechanical properties (*e.g.*, higher modulus of elasticity, as well as greater compressive and bending strength) and their aesthetic qualities, including refined texture, distinct grain, and chromatic variation (Konnerth *et al.* 2016; Morin-Bernard *et al.* 2020a, 2021), which may lead to final glulam with smaller cross-sections or higher load-carrying capacities (Silva *et al.* 2024). The growing shift toward hardwood utilization is further driven by socio-economic and environmental incentives, including the strategic valorization of underutilized hardwood resources, economic support for regional silviculture operations, alignment with afforestation and biodiversity conservation policies, and the emerging scarcity of softwood feedstock caused by climatic changes, pest infestations, and rising demand (Morin-Bernard *et al.* 2020a; Satir *et al.* 2024).

Yellow birch (*Betula alleghaniensis* Britt.) is a promising hardwood species for glulam production in Canada, representing 12.1% of the Annual Allowable Cut (AAC) for hardwoods in the province of Quebec alone. Yellow birch typically exhibits a density between 608 and 649 kg/m³, a modulus of elasticity (MOE) ranging from 10,600 to 14,100 MPa, and a modulus of rupture (MOR) between 56.8 and 106 MPa (Jessome 2000). Notably, Quebec accounts for approximately half of the country's total hardwood AAC, further underscoring yellow birch's strategic potential in regional and national engineered wood manufacturing (Bureau du Forestien en Chef 2020). Morin-Bernard *et al.* (2021) verified that the strength of yellow birch finger joint exceeded the tensile strength requirement for SPF-selected structural from NLGA SPS-1, despite the failure mode being attributed to adhesive failure. Similar bonding characteristics were observed for European Silver Birch (*Betula pendula* Roth) finger joints and CLT (Stolze *et al.* 2023; Gašparík *et al.* 2024). Considering yellow birch's widespread use in plywood manufacturing, research has largely concentrated on this product category, leaving its potential in other engineered wood products (EWPs), such as glulam, relatively unexplored (Jungerstam 2023).

Since large-diameter logs are typically used for plywood, carpentry, and wood flooring, smaller logs may offer a viable alternative for incorporating this species into glulam production. Lux *et al*. (2025) proposed a solution for low-quality European beech (*Fagus sylvatica* L.) and oak (*Quercus* spp.), utilizing a method known as Strip-Like Laminations (SLL). An SLL is a lamella produced by face-bonding small wood sections in a way that defects are randomly distributed along its length. Careful attention is required to ensure that adjacent sections are not sourced from the same original plank. The authors demonstrated that the mechanical properties of these lamellae were homogenized compared to traditional solid wood lamellae, enabling the use of more than three quarters of the produced SLLs for structural applications. However, their performance in full-scale glulam elements was not evaluated.

The aim of this study was to evaluate the effect of Strip-Like Laminations (SLL) made from yellow birch (*Betula alleghaniensis* Britt.) used as external layers in full-scale glulam elements. The objective was to assess the degree of homogenization in bending performance and to analyze the effects and challenges associated with face-bonding SLLs. It was hypothesized that incorporating SLLs would reduce variability in bending strength by redistributing natural defects and promoting more uniform stress distribution, while maintaining overall structural capacity.

EXPERIMENTAL

Materials

The wood species used in this study was grade No. 2 yellow birch (*Betula alleghaniensis* Britt.), locally known as Merisier, sourced from a local mill in the Québec Province, Canada. The planks, with initial dimensions of 2.8 m × 127 mm × 24 mm (length, width, and thickness), were conditioned for three weeks in a climate-controlled room at 20 °C and 65% relative humidity prior to glulam production. To characterize the material according to ASTM D143 (2023), a total of 34 small specimens (101.6 mm × 25.4 mm × 25.4 mm) were extracted from the wood batch. After conditioning, yellow birch exhibited an average density of 680 kg/m³ (CoV = 8.8%), a compressive strength parallel to the grain of 47.3 MPa (CoV = 6.7%), and a moisture content of 11%.

The adhesive used for glulam production was LOCTITE HB X602 PURBOND NA, a one-component polyurethane, while the primer applied to prepare the lamellae surfaces was LOCTITE PR 3105 PURBOND. Both products were supplied by Henkel Adhesives.

Glue Laminated Timber Production

Glulam production was divided into two stages: the fabrication of SLLs and the assembly of the glulam beams. Initially, small-section strips measuring 2.3 m × 50 mm × 24 mm were extracted from the original planks and planned down to a thickness of 20 mm. Planning occurred on the same day as bonding with time interval of less than 3 hours between both procedures. The orientation of strips was done using the same procedure of Lux *et al*. (2025), explained in the Introduction section. An example of how the strips were positioned for SLL production can be seen in Fig. 1.

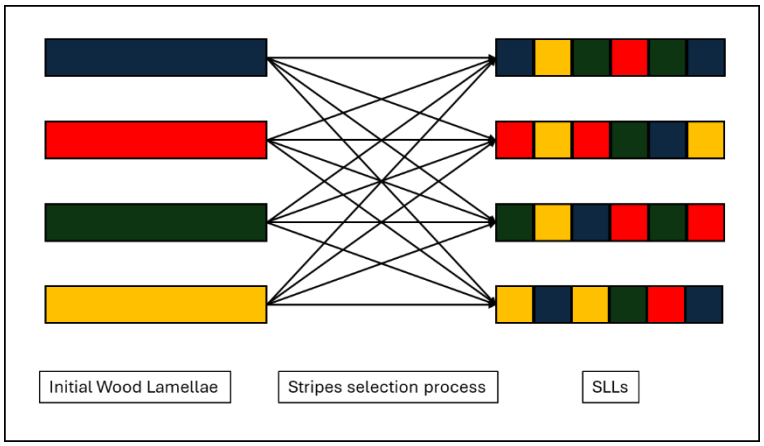

Fig. 1. Schematic of strips positioning in SLLs production

A water-diluted primer solution (1:10) was applied to the broad surfaces of the laminations by manual pulverization to ensure uniform product distribution (approximately 20 g/m²), as recommended by the manufacturer. Film thickness and primer uptake were not measured, as these analyses were beyond the scope of the present study. After a one-hour waiting period, adhesive was spread using a V-type adhesive spreader with a 6 mm (¼") opening, achieving a glue spread weight per unit area of approximately 140 g/m² as recommended by the manufacturer. SLLs were produced by bonding six of these small sections together in a Doucet 1620 mechanical press (Daveluyville, Canada) for a

minimum of five hours. Pressure was applied *via* 14 threaded rods and nuts (25.4 mm diameter), evenly distributed along the length of the element to ensure uniform pressure distribution. A cordless impact wrench with a maximum torque of 542 N·m was used to tighten the nuts. Each bonded element was conditioned in a climate-controlled room at 20 °C and 65% relative humidity for seven days before being cut in half with a circular saw to produce two SLLs.

The glulam beam production process followed the same principles used for fabricating SLLs, with the beams consisting of six layers measuring 2.3 m × 120 mm × 20 mm each. Three glulam beams were produced and tested for each design (see Fig. 2), except for the WD4 configuration, for which only one beam was evaluated. Wood lamellae were visually classified into two categories based on the presence of knots, cracks, bark inclusions, and deformations, following the common classification method of hardwoods in Canada (Morin-Bernard *et al.* 2020b). Lamellae free from visible defects were used in the traditional configuration (DF), while those with imperfections were utilized in the remaining designs. It is important to note that the visual classification doesn't necessarily relate to the lamellae mechanical performance (Bencsik *et al.* 2025). The beams were then cut and planned to final dimensions of 2.25 m × 115 mm × 120 mm prior to testing. Finger joints were intentionally excluded from this study to eliminate their potential influence on the evaluated variables; therefore, all lamellae were cut down from 2.8 m to 2.3 m.

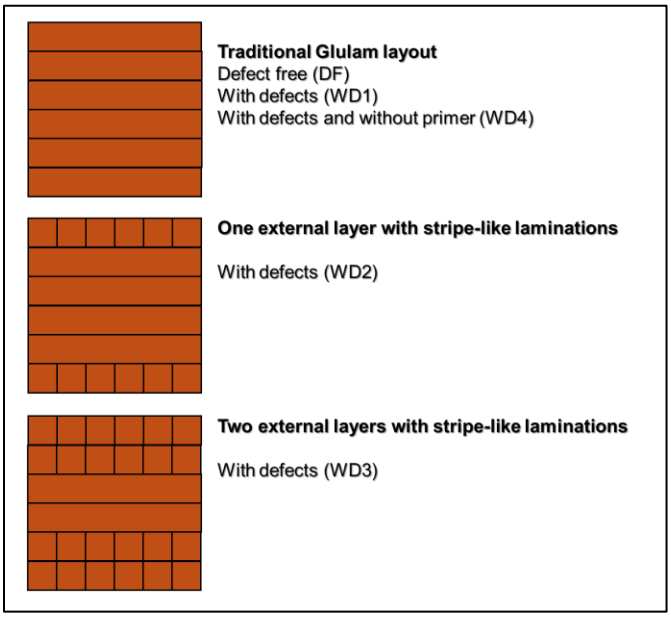

Fig. 2. Glulam beams with strip-like laminations experimental design

Testing Methodologies

Four types of characterization were performed on the yellow birch (*Betula alleghaniensis* Britt.) glulam specimens. First, the beams underwent mechanical testing using a four-point bending method. Following breakage, samples for bonding quality evaluation were extracted from undamaged sections at the ends of the beams. The methodologies and equations applied in this study are presented in the following subsections. While theoretical and numerical analysis of the beams could provide an interesting point in comparison with the experimental results, such an investigation was beyond the scope of this study and is suggested as a direction for future work.

Four-point bending

Each beam was tested using the four-point bending method, in accordance with ASTM D198 (2022). A Tinius Olsen 444k universal testing machine (Tinius Olsen Test Machine Company, Horsham, PA, USA) was employed for the tests. The span length was 2160 mm, with the loading heads positioned at one-third intervals along the span. Loading was applied at a constant rate of 6.3 mm/min, and failure occurred between 6 and 20 minutes, as specified by the standard.

Prior to testing, a preload of approximately 900 N was applied to ensure contact between the loading apparatus and the specimen. Vertical displacement at the beam's center was measured using laser transducers placed on each side, with a maximum displacement measuring capacity of 55 mm. The apparent modulus of elasticity was determined within the linear portion of the force *vs.* displacement curve, specifically between loads of 6 and 24 kN, as calculated using Eq. 1,

$$MOE_{app} = 1.012\ (23Pl^3/108bd^3D) \quad (1)$$

where MOE_{app} is the apparent modulus of elasticity (MPa), P is the increment if the load on the linear-elastic deflection of the beam (N), l is the distance between supports (mm), b is the beam's width (mm), d is the height, and D is the deflection caused by the increment of P (mm).

The coefficient 1.012 was extracted from NLGA SPS 2 (2024), based on the span-to-depth ratio of 18 in the tested beams. This ratio was selected because the maximum beam length was limited by the press dimensions during glulam production. Finally, the modulus of rupture was calculated using the maximum load sustained by each beam prior to failure, as outlined in Eq. 2,

$$MOR = P_{max}l/bd^2 \quad (2)$$

where MOR is the modulus of rupture (MPa) and P_{max} is the maximum load resisted by the specimen before failure (N).

Block shear strength

Block shear tests were conducted in accordance with CSA O122 (2021). Ten specimens were extracted from each beam previously tested in bending, with each specimen comprising only the two external layers, resulting in a total of 130 specimens. Each specimen measured 50 mm × 50 mm × 38 mm and featured a 5 mm notch on both sides. The contact area between lamellae was measured using a caliper with 0.01 mm resolution after conditioning for 7 days at 20 °C and 65% RH. Shear testing was performed using an MTS QTest load frame (Eden Prairie, USA) equipped with a 50 kN load cell and a compression shearing tool, operating at a testing speed of 5.0 mm/min. This was the same as used by Silva *et al.* (2025). Block shear strength was calculated using Eq. 3,

$$BS = P_{max}/S \quad (3)$$

where BS is the block-shear strength (MPa) and S is the bonded area of the specimen (mm²).

A visual assessment of the fractured surfaces of the specimens was carried out to quantify the percentage of area that failed in wood, referred to as wood failure percentage (WFP).

Delamination

Delamination tests were conducted following the CSA O122 (2021) standard. Three specimens measuring 75 mm x 115 mm x 120 mm were extracted from each beam previously tested in bending, yielding a total of 39 specimens. Initial mass and glue line length, at the end grain direction, were recorded after conditioning the samples for seven days under the same climate-controlled conditions used for the glulam beams.

The specimens were submerged in water at room temperature and placed inside a Wood Treatment Technology (WTT) impregnation cylinder (Grindsted, Denmark), which offers computer-controlled vacuum and pressure capabilities. The delamination procedure included a single cycle consisting of a 30-minute vacuum at 70 to 85 kPa, followed by a two-hour pressure phase at 480 to 550 kPa. After treatment, specimens were oven-dried at 65 °C for 10 to 15 hours until their mass increased to between 112% and 115% of the original conditioned mass.

Total delamination was calculated according to Eq. 4,

$$D_t = 100(l_1/l_2) \quad (4)$$

where D_t is the total delamination (%), l_1 is the sum of the delaminated length of the specimen (mm), and l_2 is the sum of the length of all glue lines of the specimen (mm).

Statistical Analysis

Statistical analyses were conducted to compare the averages obtained for MOE_{app}, MOR, BS, and D_t. Data normality was assessed using the Shapiro-Wilk test, and variance was analyzed using Tukey's test at a 5% significance level, with support from R software (version 4.3.2).

RESULTS AND DISCUSSION

The bending and bonding performance of yellow birch (*Betula alleghaniensis* Britt.) glued laminated timber (glulam) is summarized in Table 1. Beams with WD1, WD2, and WD3 designs exhibited comparable mechanical properties, while DF beams demonstrated greater stiffness (MOE_{app}), resulting in reduced displacement before reaching peak load capacity. This enhanced stiffness in DF design highlights the influence of structural imperfections on mechanical behavior. The slightly lower stiffness observed in WD2 and WD3 appears related to the presence of strip-like laminations (SLLs), which introduced fiber discontinuities between adjacent strips. Nevertheless, the MOE_{app} values obtained in this study remain within the range reported for yellow birch from New Brunswick, Canada, where average MOE was 10,954 MPa (ranging from 4,064 to 14,985 MPa) and MOR averaged 106.5 MPa (ranging from 44.2 to 136.7 MPa) (Duchesne *et al.* 2016). These results confirm that, despite design variations, the performance of glulam beams incorporating SLLs aligns with established benchmarks for the species.

The stiffness variability observed in WD2 beam models was higher, with standard deviation values exceeding those of WD1 and WD3 by more than a factor of two. This variation may reflect production challenges that also influenced bonding performance, as discussed below. The higher standard deviation observed in WD2 models can be attributed to the interaction between bonding irregularities and wood defects.

Table 1. Bending and Bonding Results of Yellow Birch Glulam

Properties	DF	WD1	WD2	WD3	WD4
MOE_{app} [MPa]	14666a* (4.01%)**	12873b (2.20%)	13019b (6.35%)	12650b (3.30%)	12003***
MOR [MPa]	83.76a (13.82%)	80.72a (14.02%)	83.66a (5.32%)	81.68a (5.00%)	62.58***
BS Strength [MPa]	20.31a (13.44%)	19.16a (9.66%)	14.69b (22.94%)	14.60b (20.27%)	14.12b (12.18%)
WFP [%]	89.52a (22.22%)	84.33ab (19.05%)	73.50bc (36.49%)	68.50c (29.88%)	6.00d (35.00%)
BS success rate [%]	96.7	100	90	96.7	0.0
D_t [%]	6.50a (64.84%)	6.31a (79.67%)	8.46a (79.33%)	9.93a (94.35%)	86.35b (16.50%)
Maximal Delamination [%]	33.92	34.90	50.32	39.47	100

* Same letter in a row means no significant difference (p-value > 0.05).
** Values between parenthesis are the coefficients of variation of the sample.
*** Results obtained for a single specimen.

The strip configuration introduces multiple bonded interfaces, which increases the likelihood of adhesive thickness variations and incomplete contact during assembly. These inconsistencies affect stress transfer efficiency between adjacent strips, leading to localized stiffness reductions. Additionally, wood natural defects such as grain deviation and micro-cracks disrupt load paths and can create non-uniform stress fields under bending. The combined effect of adhesive heterogeneity and the raw material nature explain the greater dispersion in apparent modulus of elasticity MOE_{app} for WD2 compared to WD1 and WD3. These factors contributed to the mechanical response diversity observed across WD2 samples. Nevertheless, the maximum coefficient of variation (CoV) for apparent modulus of elasticity (MOE_{app}) remained below 7%, indicating relatively low data dispersion. This level of dispersion was well within acceptable limits, considering that CoV values for certain wood elastic properties can reach 21% or more under specific conditions (Legrais *et al.* 2025).

Additionally, the WD4 beam, which lacked primer application before gluing, showed a tendency toward reduced strength and stiffness. As illustrated in Fig. 3a, failure in WD4 occurred through tensile rupture of the two lower lamellae and shear failure along the central glue line at the neutral axis. These observations highlight the importance of surface preparation, through primer application, and provide valuable guidance for improving bonding reliability in future designs. It should be noted that WD4 was not tested in triplicate like the other configurations and, therefore, it represents a limitation of the present study.

The test results demonstrated that the modulus of rupture (MOR) across beam combinations was statistically comparable, with no significant differences detected between traditional beams and those constructed using SLLs. This finding suggests that integrating SLLs as external layers can maintain structural strength while offering an alternative approach for material utilization.

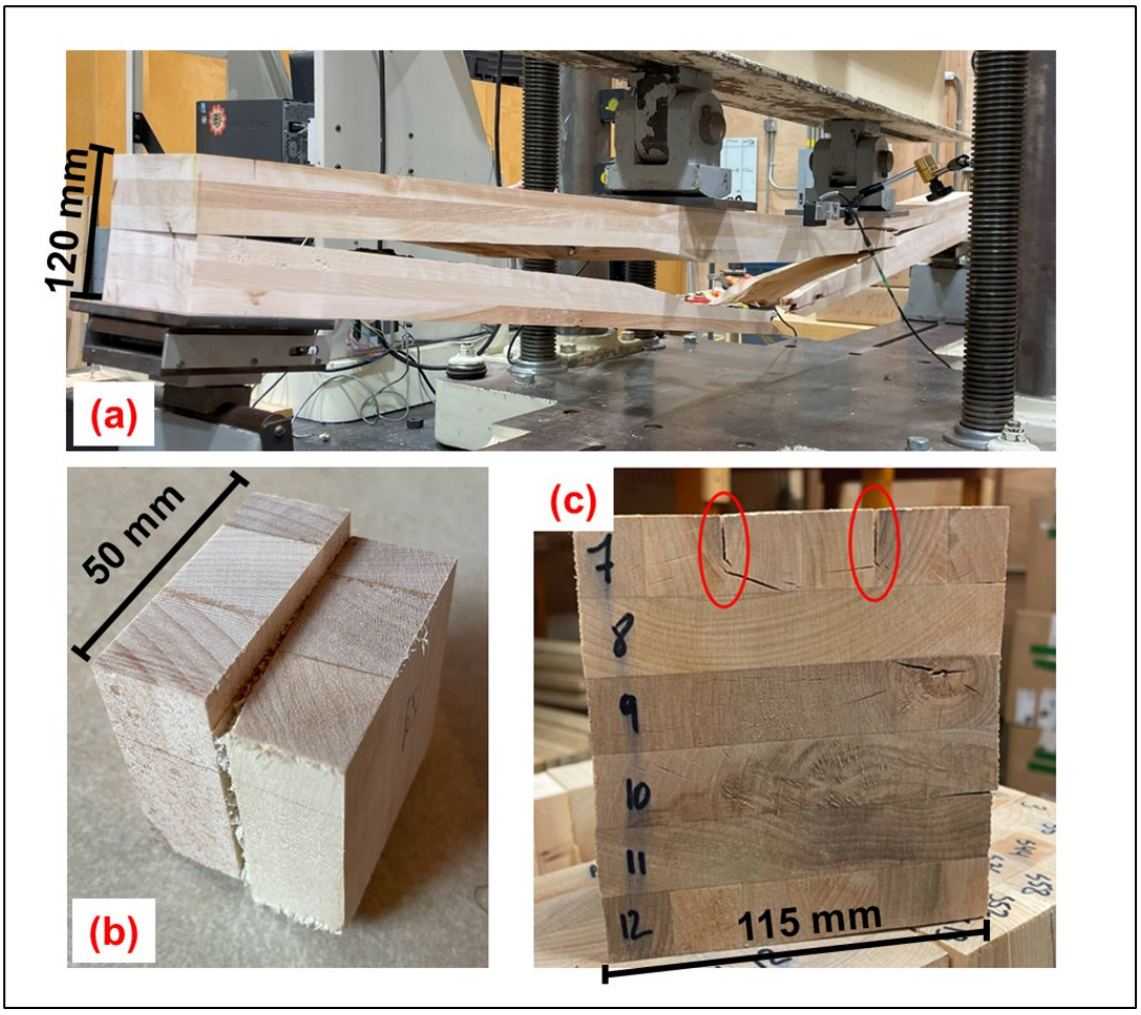

Fig. 3. (a) Neutral plane shear failure during bending test of the non-primed bonded glulam beam; (b) Voids between bonded strip laminations; and (c) In-layer delamination between strips.

A principal outcome of this study is the marked reduction in variability of bending strength when Strip-Like Laminations (SLLs) were employed as external layers. Beams WD2 and WD3 exhibited coefficients of variation as low as 4.45%, compared to values exceeding 13.82% for DF and WD1, which represents a reduction of more than threefold. This improvement in performance consistency is significant for structural reliability and design optimization because reduced variability enhances predictability and allows for more efficient material utilization. The observed reduction in variability can be attributed to the mechanical behavior introduced by lamellar discontinuity in SLLs. By segmenting the lamellae and bonding smaller sections, SLLs interrupt the continuity of natural defects such as knots or grain deviations, preventing the formation of critical stress concentrations. This discontinuity promotes a more uniform stress distribution under bending loads because localized weaknesses are dispersed across multiple bonded interfaces rather than concentrated in a single region. Consequently, the bending response becomes less sensitive to the inherent heterogeneity of hardwood, leading to improved consistency in strength performance. Lux *et al.* (2025) observed CoVs varying from 19% for beech and 22% for oak in flatwise bending MOR for single SLLs. Therefore, the degree of homogenization observed for glulam was higher than those of single lamellae. So far, only Lux *et al.* (2025)

have evaluated SLL technique, underscoring both the novelty of the present work and the need for further research on the subject. MOR CoV of *Populus tremuloides* (Michx) glulam, which is another type of hardwood found in Québec province, was on average 27.2% (Legrais *et al.* 2025), showing that yellow birch is intrinsically a more homogeneous species.

As shown in Table 1, there was a slight reduction in strength when a second lamella incorporating SLL was introduced (*i.e.*, design W3). This decrease in performance may be linked to production-related inconsistencies that were also identified during block-shear testing procedures (Fig. 3b). Although Fig. 3b illustrates the presence of voids and vertical delamination, their frequency and average area were not quantified in this study. Future investigations should increase the width of small section strips before bonding to avoid this issue. The block-shear tests revealed that beams manufactured from simple, defect-free lamellae demonstrated the highest strength values. Specifically, the DF glulam yielded an average shear strength of 20.31 MPa, closely followed by the WD1 glulam with an average of 19.16 MPa, suggesting comparable mechanical performance between the two.

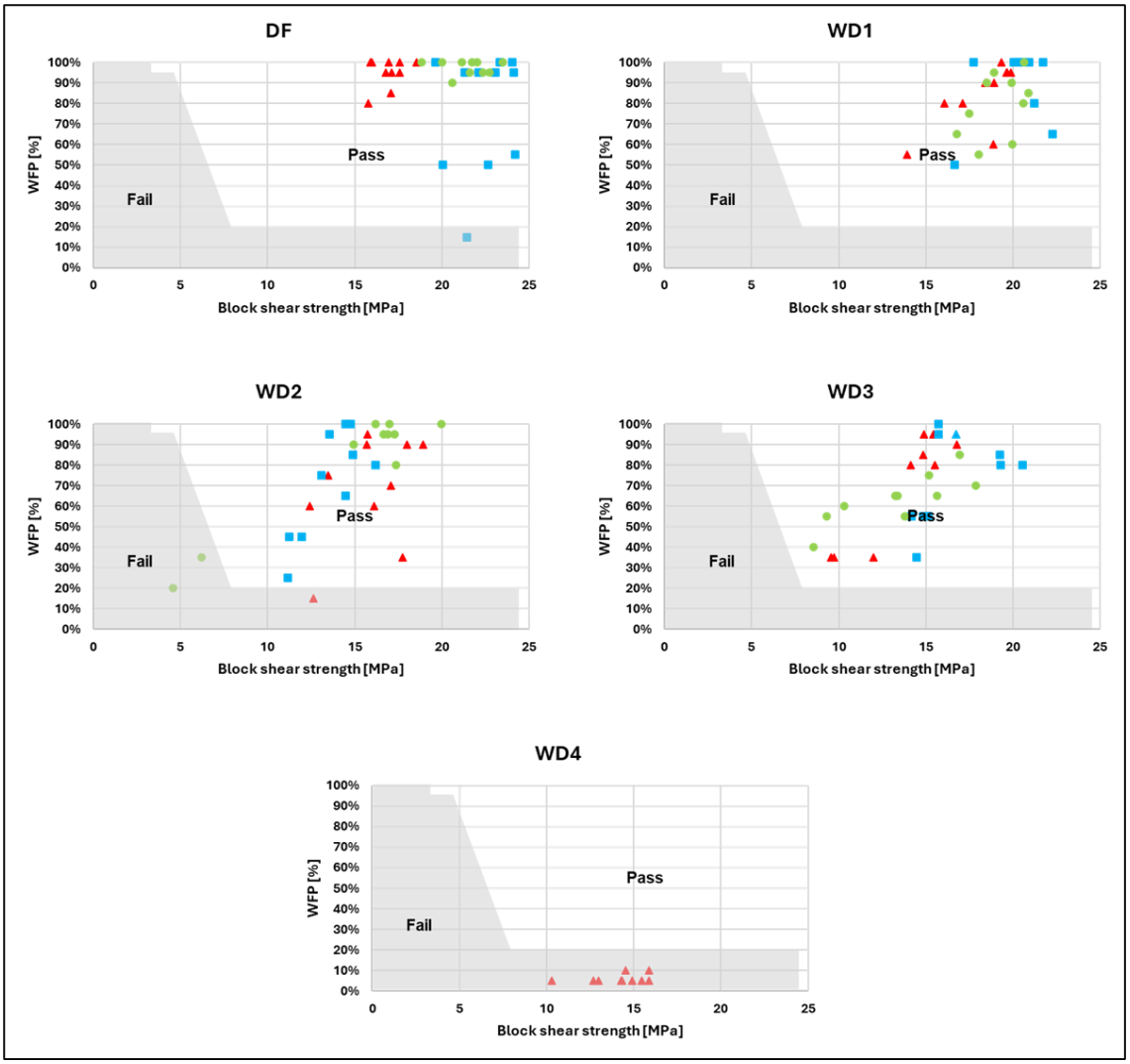

Fig. 4. Fail-pass diagrams for the block shear performance evaluation

Figure 4 presents a pass/fail assessment for the tested beams, where most specimens fell within the pass category, consistent with the values listed in Table 1, apart from WD4. Average wood failure percentage (WFP) ranged from 89% to 68% in primer-bonded glulam, but it dropped to only 6% in WD4, highlighting the severe reduction in bonding quality when no primer was applied. These findings align with those reported by Silva *et al.* (2024), who observed similar reductions in mechanical performance in non-primed bonded hardwoods compared to counterparts that underwent surface treatment prior to bonding. The benefits of surface preparation on hardwoods were also studied by Leggate *et al.* (2021, 2022), which verified that adhesives generally penetrate less these species while creating voids in the adhesive zone.

Table 1 also indicates no statistically significant difference in block-shear performance among designs WD2, WD3, and WD4, all exhibiting average shear strengths of approximately 14 MPa. A slight downward trend from WD2 to WD3 suggests a gradual decline in this property, likely associated with production challenges in SLL fabrication. Specifically, gluing 50 mm wide lamellas did not consistently ensure uniform strip formation across the 20 mm thickness of the beam, occasionally creating localized voids where surfaces failed to achieve full contact (Fig. 3b). Despite these inconsistencies, most beams met performance expectations, with further analysis in Fig. 4 highlighting that only WD4 exhibited 100% of samples in the "fail" zone. This outcome underscores the critical role of primer application in bonding effectiveness as previously discussed.

According to CSA O122 (2022), the permissible delamination across a specimen's glue line must not exceed 10% of the total length of the bonded surface. As illustrated in Fig. 5, several specimens surpassed this threshold, revealing areas for improvement in bonding consistency. At least one sample of each combination had total delamination over the standard threshold. This requirement represents a key challenge when applying hardwoods in engineered wood products, particularly compared to softwoods. Unlike softwoods, hardwoods such as yellow birch exhibit a diffuse-porous structure with smaller and less continuous lumens, as well as higher extractive content, which limits adhesive penetration and reduces mechanical interlocking within the cell structure. These anatomical features, combined with the presence of strip-like laminations (SLLs) and natural defects, increase the likelihood of incomplete wetting and weak boundary layers, ultimately leading to higher delamination rates. Figure 5 and Table 2 show a trend of increased delamination with the introduction of defects and the addition of strip-like laminations (SLLs), accompanied by greater variability in results. These observations are consistent with previous studies on hardwood bonding challenges (Boku *et al.* 2023; Silva *et al.* 2024), especially for yellow birch (Tree Canada 2025). Optimization of surface preparation and adhesive strategies will be essential to ensure reliable performance and enable industrial-scale application of this material.

Figure 3c highlights the presence of vertical delamination in models incorporating SLLs, a phenomenon not currently addressed by standardized delamination criteria. Vertical delamination was not measured; however, it can be seen in Fig. 3c that it surpassed half of the SLL bonded length. While this type of delamination may increase exposure of internal wood surfaces to environmental agents and potentially affect long-term durability, its identification provides valuable insight for improving design and bonding strategies. Among all configurations, WD4 exhibited the highest extent of delamination, an outcome associated with the absence of primer prior to adhesive application. This finding reinforces the critical importance of surface treatment in achieving reliable bonding performance and offers a clear pathway for enhancing the durability of SLL-based glulam beams.

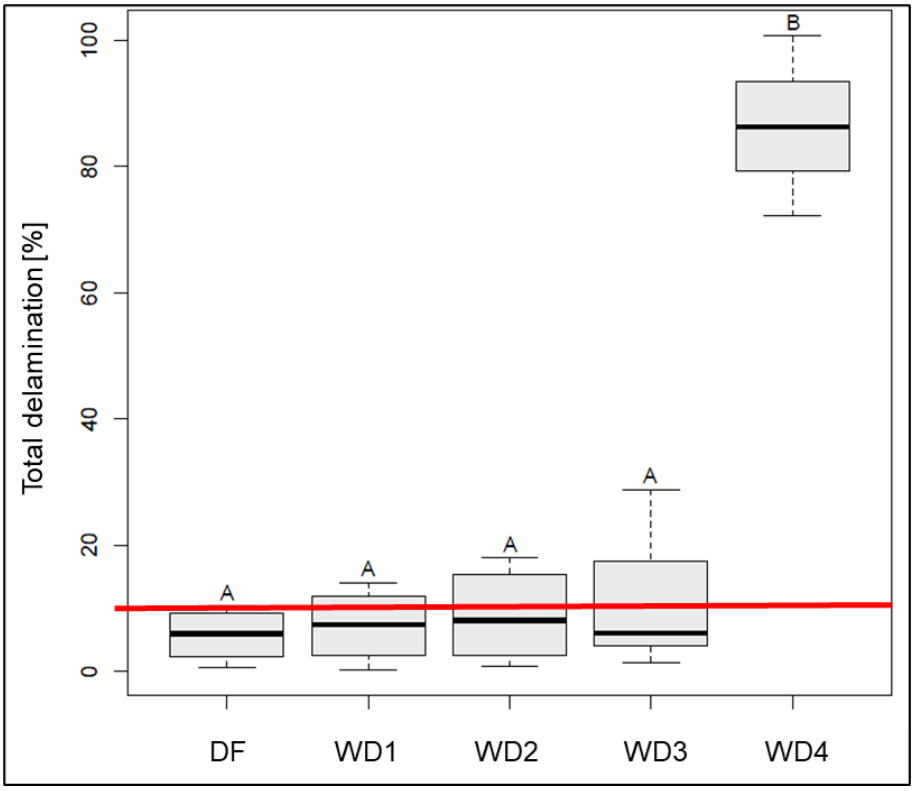

Fig. 5. Total delamination of yellow birch (*Betula alleghaniensis* Britt.) glulam samples

CONCLUSIONS

1. The incorporation of strip-like laminations (SLLs) in models WD2 and WD3 resulted in modulus of rupture (MOR) values comparable to those of conventional glulam designs, while significantly reducing variability. Notably, the standard deviation was approximately one-third of that observed in traditional specimens, indicating improved uniformity in mechanical performance.
2. Adhesive performance in block-shear tests was satisfactory; however, issues arose regarding delamination resistance. The inclusion of SLLs appeared to worsen delamination (increasing it up to 9.93%), highlighting the need for optimized manufacturing protocols for these elements.
3. Natural defects of wood had a negative impact on the apparent modulus of elasticity (MOE_{app}) of the glulam specimens (with reductions ranging from about 1600 MPa to 2000 MPa depending on the configuration) and the replacement of external layers with SLLs did not alter this property.
4. The application of primer proved to be essential for improving bonding effectiveness of yellow birch (*Betula alleghaniensis* Britt.). Without it, wood failure percentage (WFP) values dropped significantly, around 6%, and delamination rates rose sharply, occasionally leading to complete separation of the layers.

Future work should focus on quantifying vertical delamination to better evaluate structural integrity, optimizing strip width and adhesive penetration to enhance bonding performance, and assessing the long-term durability of SLL-based glulam beams under varying environmental exposures. These directions would provide deeper insights into material behavior, improve manufacturing efficiency, and validate the reliability of SLL-based systems for practical applications.

ACKNOWLEDGMENTS

The authors are thankful to Natural Sciences and Engineering Research Council (NSERC) of Canada for the financial support through its IRC and CRD programs (IRCPJ 461745–18 and RDCPJ 524504–18).

REFERENCES CITED

ASTM D143-22 (2023). "Standard test methods for small clear specimens of timber," ASTM International, West Conshohocken, PA.

ASTM D198-22 (2022). "Standard test methods of static tests of lumber in structural sizes," ASTM International, West Conshohocken, PA.

Bencsik, B., Denes, L., Hassler, C. C., Norris, J. R., and McNeel, J. F. (2025). "Relationship between timber grade and local, global, and dynamic modulus of elasticity in red oak and red maple structural lumber," *BioResources.* 20(2), 2609-2627. https://doi.org/10.15376/biores.20.2.2609-2627

Boko, I., Glavinić, I. U., Torić, N., Hržić, T., Vranković, J. L., and Abramović, M. (2023). "Potential of hardwoods harvested in Croatian forests for the production of glued laminated timber," *Int. J. Struct. Civ. Eng. Res.* 12(4), 131-134. https://doi.org/10.18178/ijscer.12.4.131-134

Bureau du Forestien en Chef (2020). "Détermination 2018-2023 Synthèse provinciale," (https://forestierenchef.gouv.qc.ca/wp-content/uploads/Synthese_provinciale_mod_mai2020.pdf), Accessed 23 July 2025. [in French]

CSA-O122-16 (2021). "Structural glued-laminated timber," CSA Group, Toronto, ON.

Duchesne, I., Vincent, M., Wang, X., Ung, C. H., and Swift, D. E. (2016). "Wood mechanical properties and discoloured heartwood proportion in sugar maple and yellow birch grown in New Brunswick," *BioResources* 11(1), 2007-2019. https://doi.org/10.15376/biores.11.1.2007-2019

Gašparík, M., Das, S., Kytka, T., Karami, E., Bahmani, M., and Sviták, M. (2024). "Bonding characteristics of CLT made from silver birch (*Betula pendula* Roth.), European aspen (*Populus tremula* L.) and Norway spruce (*Picea abies* (L.) H. Karst.) wood," *Forests* 15, article 1656. https://doi.org/10.3390/f15091656

Jessome, A. (2000). *Strength and Related Wood Properties of Wood Grown in Canada*, Eastern Forest Product Laboratory, Ottawa, Canada.

Jungerstam, I. (2023). *Experimental Investigation of the Rolling Shear Properties of Birch Timber*, Master's Thesis, Aalto University, Espoo, Otaniemi, Finland.

Konnerth, J., Kluge M., Schweizer G., Miljković M. and Gindl-Altmutter W. (2016). "Survey of selected adhesive bonding properties of nine European softwood and hardwood species," *Eur. J. Wood Wood Prod.* 74, 809-819. https://doi.org/10.1007/s00107-016-1087-1

Leggate, W., Shirmohammadi, M., McGavin, R. L., Outhwaite, A., Knackstedt, M., and Brookhouse, M. (2021). "Examination of wood adhesive bonds via MicroCT: The influence of pre-gluing surface machining treatments for southern pine, spotted gum, and Darwin stringybark timbers," *BioResources* 16(3), 5058-5082. https://doi.org/10.15376/biores.16.3.5058-5082

Leggate, W., Outhwaite, A., McGavin, R. L., Gilbert, B. P., and Gunalan, S. (2022). "The effects of the addition of surfactants and the machining method on the adhesive bond quality of spotted gum glue-laminated beams," *BioResources* 17(2), 3413-3434. https://doi.org/10.15376/biores.17.2.3413-3434

Legrais, O. E. G., Blanchet, P., Boudaud, C., Cogulet, A., and Silva, J. V. F. (2025). "Assessment of *Populus tremuloides* (Michx) mechanical characteristics for glulam production," *Mater. Struct.* 58(51), 1-16. https://doi.org/10.1617/s11527-025-02585-1

Lux, S., Konnerth, J., and Neumüller, A. (2025). "Mechanical properties of strip-like laminations made from hardwood," *Eur. J. Wood Wood Prod.* 83(90), 1-13. https://doi.org/10.1007/s00107-025-02246-8

Morin-Bernard, A., Blanchet, P., Dagenais, C., and Achim, A. (2020a). "Use of northern hardwoods in glued-laminated timber: A study of bondline shear strength and resistance to moisture," *Eur. J. Wood Wood Prod.* 78, 891-903. https://doi.org/10.1007/s00107-020-01572-3

Morin-Bernard, A., Blanchet, P., Dagenais, C., and Achim, A. (2020b). "Strength grading of northern hardwood species for structural engineered wood products: Identification of the relevant indicating properties," *BioResources* 15(4), 8813-8832. https://doi.org/10.15376/biores.15.4.8813-8832

Morin-Bernard, A., Blanchet, P., Dagenais, C., and Achim, A. (2021). "Glued-laminated timber from northern hardwoods: Effect of finger-joint profile on lamellae tensile strength," *Constr. Build. Mater.* 12(2), 153-162. https://doi.org/10.1016/j.conbuildmat.2020.121591

NLGA SPS 2 (2024). "Special products standard for machine graded lumber," National Lumber Grades Authority, Ottawa, ON.

Satir, E., Adhikari, S., and Hindman, D. P. (2024). "Evaluation of bending and shear properties of mixed softwood & hardwood cross-laminated timbers," *J. Build. Eng.* 96, article 110646. https://doi.org/10.1016/j.jobe.2024.110646

Silva, J. V. F., Blanchet, P., and Cogulet, A. (2024). "Bonding performance of Canadian hardwoods to produce glued laminated timber," *J. Build. Eng.* 98, article 111389. https://doi.org/10.1016/j.jobe.2024.111389

Silva, J. V. F., Cogulet, A., Blanchet, P., and Pechon, Q. (2025). "Effect of relative humidity level on bonding properties of black spruce glulam," *BioResources* 20(2), 2922-2932. https://doi.org/10.15376/biores.20.2.2922-2932

Stolze, H., Gurnik, M., Kagel, S., Bollmus, S., and Militz, H. (2023). "Determination of the bonding strength of finger joints using a new test specimen geometry," *Processes* 11, article 445. https://doi.org/10.3390/pr11020445

Subhani, M. and Lui, H. Y. (2024). "Effect of primer and fibre orientation on softwood–hardwood bonding," *J. Compos. Sci.* 8, article 192. https://doi.org/10.3390/jcs8060192

Tree Canada (2025). Canada's Arboreal Emblems: Quebec — Yellow birch (*Betula alleghaniensis*)," (https://treecanada.ca/resources/canadas-arboreal-emblems/yellow-birch/), accessed 23 July 2025.
Van Acker, J. (2021). "Opportunities and challenges for hardwood based engineered wood products," in: *9th Hardwood Proceedings*, Sopron, Hungary, pp. 5-14.

Article submitted: October 24, 2025; Peer review completed: November 8, 2025; Revised version received and accepted: January 16, 2026; Published: January 23, 2026.
DOI: 10.15376/biores.21.1.2215-2228